Autoresonant Excitation of Antiproton Plasmas

G. B. Andresen *et al.* (ALPHA Collaboration)

LY12041

Autoresonant Excitation of Antiproton Plasmas

G.B. Andresen,[1] M. D. Ashkezari,[2] M. Baquero-Ruiz,[3] W. Bertsche,[4] P.D. Bowe,[1] E. Butler,[4] P. T. Carpenter,[5] C.L. Cesar,[6] S. Chapman,[3] M. Charlton,[4] J. Fajans,[3] T. Friesen,[7] M.C. Fujiwara,[8] D.R. Gill,[8] J.S. Hangst,[1] W.N. Hardy,[9] M.E. Hayden,[2] A.J. Humphries,[4] J. L. Hurt,[5] R. Hydomako,[7] S. Jonsell,[10] N. Madsen,[4] S. Menary,[11] P. Nolan,[12] K. Olchanski,[8] A. Olin,[8] A. Povilus,[3] P. Pusa,[12] F. Robicheaux,[5] E. Sarid,[13] D.M. Silveira,[14] C. So,[3] J.W. Storey,[8] R.I. Thompson,[7] D.P. van der Werf,[4] J.S. Wurtele,[3, 15] and Y. Yamazaki[14, 16]

(ALPHA Collaboration)

[1]*Department of Physics and Astronomy, Aarhus University, DK-8000 Aarhus C, Denmark*
[2]*Department of Physics, Simon Fraser University, Burnaby BC, Canada V5A 1S6*
[3]*Department of Physics, University of California at Berkeley, Berkeley, CA 94720-7300, USA*
[4]*Department of Physics, Swansea University, Swansea SA2 8PP, United Kingdom*
[5]*Department of Physics, Auburn University, Auburn, AL 36849-5311, USA*
[6]*Instituto de Física, Universidade Federal do Rio de Janeiro, Rio de Janeiro 21941-972, Brazil*
[7]*Department of Physics and Astronomy, University of Calgary, Calgary AB, Canada T2N 1N4*
[8]*TRIUMF, 4004 Wesbrook Mall, Vancouver BC, Canada V6T 2A3*
[9]*Department of Physics and Astronomy, University of British Columbia, Vancouver BC, Canada V6T 1Z4*
[10]*Fysikum, Stockholm University, SE-10691, Stockholm, Sweden*
[11]*Department of Physics and Astronomy, York University, Toronto, ON, M3J 1P3, Canada*
[12]*Department of Physics, University of Liverpool, Liverpool L69 7ZE, United Kingdom*
[13]*Department of Physics, NRCN-Nuclear Research Center Negev, Beer Sheva, IL-84190, Israel*
[14]*Atomic Physics Laboratory, RIKEN, Saitama 351-0198, Japan*
[15]*Lawrence Berkeley National Laboratory, Berkeley, CA 94720, USA*
[16]*Graduate School of Arts and Sciences, University of Tokyo, Tokyo 153-8902, Japan*
(Dated: December 17, 2010)

We demonstrate controllable excitation of the center-of-mass longitudinal motion of a thermal antiproton plasma using a swept-frequency autoresonant drive. When the plasma is cold, dense, and highly collective in nature, we observe that the entire system behaves as a single-particle nonlinear oscillator, as predicted by a recent theory. In contrast, only a fraction of the antiprotons in a warm plasma can be similarly excited. Antihydrogen was produced and trapped by using this technique to drive antiprotons into a positron plasma, thereby initiating atomic recombination.

PACS numbers: 52.27.Jt, 52.35.Mw

Oscillators subjected to a drive with a swept frequency can become phase-locked to the drive; when this happens, the oscillator's amplitude can be controlled by varying the applied frequency. This phenomenon, called autoresonance, occurs in a variety of dynamical systems from plasma modes [1] to orbital dynamics [2]. Nonlinear oscillators can be controlled with autoresonance when one is ignorant of the oscillator's state, a fact exploited in applications from controlling Josephson-junctions [3] to mass-spectrometers [4]. This paper describes the dynamics behind the autoresonant drive that we recently used to inject antiprotons into a positron plasma, thereby forming antihydrogen that we trapped[6].

Autoresonant (AR) control requires that systems (typically uncoupled nonlinear oscillators) possess an anharmonic potential with a monotonic relationship between their response frequency and amplitude. Here we study the autoresonant excitation of a thermally broadened pure antiproton plasma. Because the total potential that results from the vacuum and plasma self-electric fields has a non-monotonic relationship between amplitude and frequency, test particles will not respond autoresonantly. Furthermore, only a subset of thermally broadened, un-

coupled test particles in the vacuum potential would have an autoresonant response. Yet we find that a charged plasma *can* behave as a single particle under autoresonant excitation despite its self-fields and thermal distribution. To our knowledge, this is the first direct confirmation of a theory developed by Barth *et al.* that claims that the repulsive self-forces cause a charged plasma to stay coherent under the autoresonance drive [5].

This paper compares the behavior of the plasma to a single particle oscillator of charge $-e$ and mass m, confined on the z-axis in an electrostatic potential with a time-varying drive electric field E_d of the form: $\Phi = -\Phi_0\big(1 - \cos(kz)\big) - E_d z \cos\big(\int \omega dt\big)$, where Φ_0, k, and E_d are parameters found by fitting to the actual potentials used in our measurements. Defining $\theta = kz$, $\bar{\epsilon}$ to be a normalized drive amplitude, and allowing the drive frequency ω to be time-dependent with a sweep (chirp) rate magnitude α, the equation of motion is:

$$\ddot{\theta} + \omega_0^2 \sin\theta = \bar{\epsilon}\cos\big(\omega_i t - \alpha t^2/2\big). \qquad (1)$$

This is the same equation as that of a uniformly driven, nonlinear pendulum with a linear (small-amplitude) os-
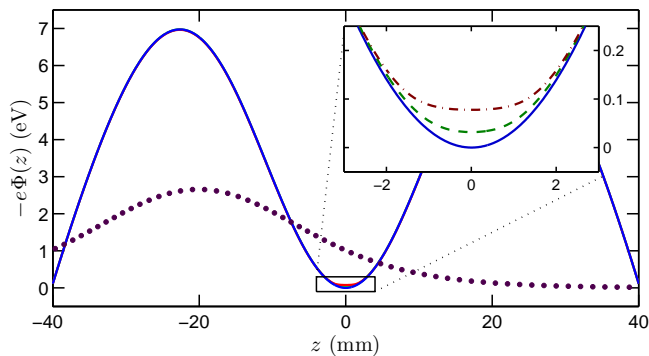
FIG. 1. (Color online) On-axis ($r = 0$) potentials used in this experiment. — Vacuum potential. $\cdots$ Typical drive potential ($\bar{\epsilon}/2\pi \sim 1.8 \cdot 10^9\,\mathrm{s}^{-2}$ scaled $\times 100$). **Inset** Total potential for the plasma ($T_\parallel = 150\,\mathrm{K}$) with - - - 15,000 ($n(0,0) \sim 6\cdot 10^{12}\,\mathrm{m}^{-3}$) and -·- 50,000 antiprotons ($n(0,0) \sim 1\cdot 10^{13}\,\mathrm{m}^{-3}$).

cillation frequency of $\omega_0 = \sqrt{ek^2\Phi_0/m}$.

On application of a *fixed* drive frequency ($\alpha = 0$), the amplitude of this oscillator beats in time, never coming to equilibrium. However, if the drive starts at an initial frequency $\omega_i > \omega_0$ and sweeps past ω_0 to a final frequency ω_f, the oscillator can phase-lock to the drive and will adjust its nonlinear frequency to match that of the drive. At a sufficiently high drive amplitude, this process will be independent of the initial conditions of the oscillator [2]. In this way, the final energy U_f of the oscillator can be chosen by ω_f through the oscillator's energy–frequency relationship. This is an autoresonant drive.

The "particle" in the actual experiment is the center-of-mass longitudinal motion of an antiproton plasma. As the dynamics of this system are governed by a many-body equation of motion [5], it is not obvious that this system's behavior can be reduced to that of a single particle.

All measurements were conducted in the ALPHA apparatus, located at the Antiproton Decelerator at CERN. ALPHA contains a minimum-B trap designed for the production and trapping of neutral antihydrogen [7] and uses Penning-Malmberg traps to catch and mix its charged constituents: antiprotons and positrons . Preparation of the antiproton plasmas followed the methods described in [8], and left the antiprotons in the potential shown in Fig. 1, in which all experiments occur.

We destructively measure the antiproton number by lowering one side of the confining potential, thereby allowing the antiprotons to escape and annihilate on the end of the trap. We count the annihilation products during this "dump" with scintillators. The two plasma conditions discussed here had approximately 15,000 and 50,000 antiprotons each, although these numbers fluctuated ($\pm 30\%$). We also imaged the radial profile of the dumped plasmas and found that in both cases their average diameter was ~ 1.6 mm [9].

The annihilation times and the potential as a function of time during a dump are used to determine the approximate longitudinal energy distribution function $f(U)dU$ of the plasma. By assuming single particle dynamics in a uniform longitudinal magnetic field and ignoring radial effects, the longitudinal energy of an antiproton is:

$$U = \frac{1}{2}mv_z^2(z) - e(\Phi(z) - \Phi(0)). \qquad (2)$$

The energy a particle has when it escapes differs from its initial energy because the dump process performs work on it. However if a particle's longitudinal action $J = \oint mv_z \cdot dz$ is adiabatically conserved, we can equate $J(t_e)$ to $J(U_0)$, and relate its escape time t_e to its energy U_0 in the well before the dump. The dumps are slow enough to dynamically preserve J in our trap, but fast compared to the antiproton-antiproton collision rate [10]. By ignoring the plasma potential and radial effects, we introduce energy errors (< 15 mV) that are much smaller than the mean energies discussed here (> 1 V). All particle distributions presented here are calculated this way.

When the plasma is in thermal equilibrium, its longitudinal temperature $T_\parallel$ can be determined by fitting an exponential to the high-energy tail of the longitudinal energy distribution, a method which can be largely insensitive to the plasma's self-fields [8, 11]. The "cold" antiproton plasmas discussed here had temperatures in the range of $(150 - 300)$ K. From the particle number, radial profile and temperature, we can calculate the plasma equilibrium density $n(r,z)$, and total potential (Fig. 1)[12].

We find the relationship of a particle energy U to a response (bounce) frequency ω_b in the potential by solving for the time τ it takes a particle to traverse the well:

$$\frac{\pi}{\omega_b(U)} = \tau(U) = \int_{z_l}^{z_r} \frac{dz}{|v_z|}, \qquad (3)$$

where v_z and the left and right turning points z_l and z_r are solved from Eq. 2 for a given potential Φ. Figure 2 plots $U(\omega_b)$, for the potentials shown in Fig. 1.

We applied a drive that chirped from a frequency ω_i that was 2.5% above ω_0 to various final frequencies ω_f's at a fixed α ($2\pi \cdot 60$ MHz s^{-1}). The resultant energy distributions were measured with 10 ms dumps performed 2 ms after the drive. As shown in Fig. 2, the mean energy of each distribution agrees with $U(\omega_f)$ calculated from Eq. 3, indicating that the bounce frequency of the plasma matched the drive frequency. This implies that the plasma response was phase-locked to the drive.

Figure 3 shows a decrease in the mean U of distributions measured at different times after applying the same drive to similar plasmas. After the excitation, parallel energy redistributes itself via collisions and can change to perpendicular motion or be lost through "evaporation" of high energy particles out of the well [8, 18]. Based on the measurements, we see that the single-particle assumption is valid for the 10 ms dumps used in the measurements.
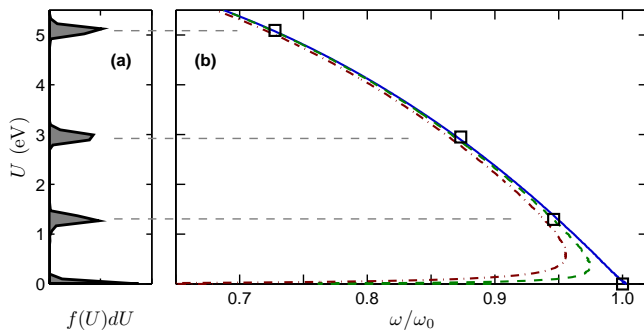
FIG. 2. (Color online) Energy versus frequency measurements and calculations (frequencies normalized to $\omega_0/2\pi = 410\,\text{kHz}$). **(a)** Distributions of $\sim 15,000$ antiprotons driven to different final frequencies. **(b)** $U(\omega_b)$ calculated from Eq. 3 for — Vacuum potential. --- Total potential with 15,000 and -·- 50,000 antiprotons (see Fig. 1). □ Mean U of each distribution plotted against its final drive frequency.
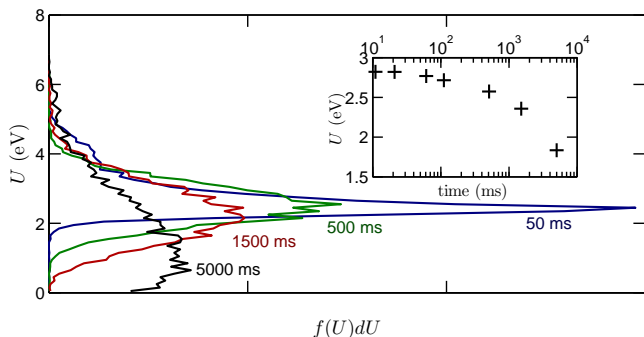

FIG. 3. (Color online) Plot of the time-evolution of the longitudinal distribution $f(U)dU$ for plasmas with $\sim 50,000$ antiprotons excited with an autoresonant drive. **Inset:** Their mean longitudinal energy as a function of the time between the autoresonant drive and the energy measurement dump.

One feature of autoresonantly-driven systems is the existence of a critical drive amplitude $\bar{\epsilon}_c$ that scales as a distinctive $\alpha^{3/4}$ power law [13]. Specifically for oscillators obeying Eq. 1, the threshold is [2]:

$$\bar{\epsilon}_c = 8\sqrt{\omega_0}\left(\frac{\alpha}{3}\right)^{3/4}. \qquad (4)$$

Above this threshold, the oscillator will lock to the drive, and the amplitude will follow the drive frequency; below the threshold, the oscillator will not lock to the drive.

This threshold is derived by modeling the phase difference between oscillator and drive as the coordinate of a "pseudoparticle" in a "pseudopotential". Phase-locking requires confinement of the pseudoparticle in a well of the pseudopotential, with a perfect phase-lock corresponding to a stationary pseudoparticle. Generally, however, the pseudoparticle oscillates around one minimum of the pseudopotential, manifesting as a modulation of the am-
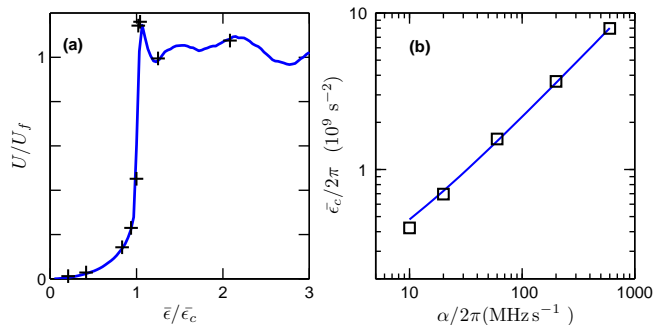

FIG. 4. (Color online) Chirp and drive amplitude threshold measurements on 15,000 antiprotons. **(a)** Amplitude threshold measurement for fixed drive parameters ($\alpha/2\pi = 200\,\text{MHz/s}$, $\omega_i/2\pi = 420\,\text{kHz}$, $\omega_f/2\pi = 360\,\text{kHz}$), with longitudinal energy U normalized to $U_f \sim 2.9\,\text{eV}$. + Mean energy of final distributions plotted against their drive amplitude and normalized to scale the threshold to 1. — Single oscillator final energy calculated as a function of drive amplitude, similarly scaled. **(b)** □ Measured $\bar{\epsilon}_c$ for a given chirp rate α. — Scaling law $\alpha^{3/4}$ (Eq. 4) fit to the data.

plitude of the real system. Near the threshold, if α is too large or $\bar{\epsilon}$ too small, the pseudopotential well will become so shallow over the course of the sweep that the pseudoparticle will escape. Thereafter, no phase-lock exists and the system's energy will remain roughly constant, even as the drive continues [2].

Experimentally, we determined the autoresonance threshold in our system by driving the plasma at different amplitudes while holding ω_i, ω_f, and α constant. The threshold amplitude $\bar{\epsilon}_c$ is the value that causes the plasma's mean energy to rise sharply. Figure 4a shows the data used to measure the threshold at $\alpha/2\pi \sim 200\,\text{MHz}\,\text{s}^{-1}$. A curve of $\bar{\epsilon}_c$ as a function of α is shown in Fig. 4b, and adheres to the scaling of Eq. 4.

We compared the threshold measurements with calculations for a single particle following Eq. 1 and found that the data agrees with the simulation after a uniform reduction of the simulation $\bar{\epsilon}$ by $\sim 20\%$ (consistent with an uncertainty in our estimate of the coupling between the drive electronics and the electrode); the blue curve in Fig. 4a includes this correction factor, and coincides with the measurements. The shape of the simulation curve is governed by details of the pseudoparticle oscillations present in the time evolution of the oscillator. In measurements of the energy after the drive, they influence the slow rise in final energy before the jump at the threshold and the fluctuations after $\bar{\epsilon}_c$. The measured data, in matching the calculations, are consistent with a pseudoparticle oscillation of the driven plasma.

These results strongly indicate that the cold plasma behaves as a single-particle oscillator under an autoresonance drive. We find, however, that a hot plasma does not respond as a single particle. We heated the cold

plasma to $T \sim 1,800\,\mathrm{K}$ by applying a strong drive near ω_0 and waited $25\,\mathrm{s}$ after the heating to allow for thermalization before applying the AR drive. We measured the capture-threshold in the manner described above. We found that, while it started following the drive at approximately $\bar{\epsilon}_c$ for the equivalent cold plasma, the hot plasma split into two distinct populations: one that followed the drive and another that remained at low energy (Fig. 5). Increasing the amplitude captured more antiprotons.

This behavior is consistent with the model proposed in [5], where it is shown that a thermal plasma will have an $\bar{\epsilon}_c$ that scales as $\alpha^{3/4}$. In the case of a high temperature and/or low density, the threshold is broad because the plasma phase space filaments during the excitation and only a fraction of the plasma (monotonically increasing with $\bar{\epsilon}$) is captured by the drive. The model further predicts that increasing the density actually narrows the transition, because the repulsive self-fields cause the plasma to act as a single particle.

Though our plasmas are not modeled exactly in [5], their behaviors follow the expected trend of the theory. Barth *et al.* define a parameter $\eta^2 = \omega_p^2/\omega_0^2$ which quantifies the importance of the self-field of the plasma ($\omega_p = \sqrt{ne^2/m\epsilon_0}$ is the plasma frequency). For instance, they find that, for a plasma with $T_\parallel \sim 2,300\,\mathrm{K}$, η^2 must be greater than ~ 4 to behave like a single particle. Our hot plasma, with $\eta^2 \sim 0.5$, has a fractional response while our cold plasma, with $\eta^2 \sim 1.6$, behaved as a single particle. Though the comparison of η^2 should be made at the same temperatures, we expect collective effects to play a more important role in our cold plasma because the its Debye length was shorter than any of its spatial dimensions, while it is longer in the case of the hot plasma [14]. We assessed the threshold behavior without collective effects for our plasmas by solving Eq. 1 for thermal ensembles (at our plasma temperatures) of non-interacting particles, and determined the capture fraction for $\bar{\epsilon}$'s around $\bar{\epsilon}_c$. Figure 5 shows that this calculation, lacking self-interactions, does not predict the sharp transition at $\bar{\epsilon}_c$ that we observe for the cold plasma.

In conclusion, we have demonstrated the controlled autoresonant excitation of the mean longitudinal energy of a thermal antiproton plasma. A cold, dense plasma behaves like a single particle oscillator, while a warm, tenuous plasma filaments under the drive, displaying a broad autoresonance threshold. This behavior is consistent with a recently published model [5].

In this paper, we have discussed finite excitation of the plasma; by extending the sweep to lower frequencies, the antiprotons can be driven out of their well and directly into a confined positron plasma [15]. These un-confined antiprotons lose phase-lock to the drive, pass through confined positrons and form antihydrogen. Many previously used methods for mixing antiprotons with positrons produced antihydrogen with too much kinetic energy to be trapped (typical traps cannot hold anti-atoms with ki-
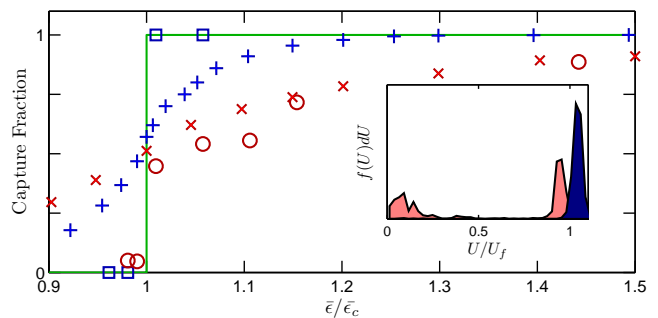

FIG. 5. (Color online) Plot of the fraction of plasma that follows the autoresonant drive ($\alpha/2\pi = 60\,\mathrm{MHz\,s^{-1}}$, $\omega_i/2\pi = 420\,\mathrm{kHz}$, $\omega_f/2\pi = 360\,\mathrm{kHz}$). $\square$ Cold plasma and $\bigcirc$ Hot plasma of 15,000 antiprotons. — Expected fraction for a single oscillator ($T_\parallel = 0\,\mathrm{K}$). $+$ Calculations for an ensemble of cold oscillators ($T_\parallel = 150\,\mathrm{K}$). $\times$ Calculations for an ensemble of hot oscillators ($T_\parallel = 1,800\,\mathrm{K}$). **Inset:** Distribution functions of an heated (pink) and an unheated (blue) plasma after the drive ($\bar{\epsilon}/\bar{\epsilon}_c \sim 1.05$).

netic energies more than $\sim 5 \cdot 10^{-5}\,\mathrm{eV}$ [7]). For example in [16], antiprotons were launched into the positrons by tipping them over a several eV barrier and produced antihydrogen measurably too warm to trap. In [17], antiprotons were heated over a few eV barrier into positrons with a fixed-frequency drive. In both cases, antiprotons entered the positrons with an excess of energy: either an initial excess of U or significant transverse energy gained from collisional energy redistribution; both reduce the likelihood of forming trappable antihydrogen [18]. In contrast, autoresonance injects the antiprotons into the positrons with little excess longitudinal energy, and if done sufficiently quickly, with minimal increase in the antiprotons' original transverse energy. Once the drive parameters were tuned tuned to those reported in [6], we found that autoresonant injection was reproducible in the face of fluctuations ($\sim 10\%$) in the number and radial profile of the initial antiproton and positron plasmas.

[1] W. Bertsche, J. Fajans, and L. Friedland, Phys. Rev. Lett., **91**, 265003 (2003).
[2] J. Fajans and L. Friedland, Am. J. Phys., **69**, 1096 (2001).
[3] O. Naaman, J. Aumentado, L. Friedland, J. S. Wurtele, and I. Siddiqi, Phys. Rev. Lett., **101**, 117005 (2008).
[4] A. V. Ermakov and B. J. Hinch, Rev. Sci. Instrum., **81**, 013107 (2010).
[5] I. Barth, L. Friedland, E. Sarid, and A. G. Shagalov, Phys. Rev. Lett., **103**, 155001 (2009).
[6] G. B. Andresen and *et al.* (ALPHA Collaboration), Nature, **468**, 673 (2010).
[7] W. Bertsche and *et al.*, Nucl. Instrum. Methods, **566**, 746 (2006).
[8] G. B. Andresen and *et al.* (ALPHA Collaboration), Phys. Rev. Lett., **105**, 013003 (2010).
[9] G. B. Andresen and *et al.* (ALPHA Collaboration), Rev. Sci. Instrum., **80**, 123701 (2009).
[10] F. F. Chen, *Introduction to Plasma Physics and Controlled Fusion Volume 1: Plasma Physics*, 2nd ed. (Plenum Press, New York, 1984).
[11] D. L. Eggleston, C. F. Driscoll, B. R. Beck, A. W. Hyatt, and J. H. Malmberg, Phys. Fluids B, **4**, 3432 (1992).
[12] S. A. Prasad and T. M. Oneil, Phys. Fluids, **22**, 278 (1979).
[13] J. Fajans, E. Gilson, and L. Friedland, Phys. Rev. Lett., **82**, 4444 (1999).
[14] C. Hansen and J. Fajans, Phys. Rev. Lett., **74**, 4209 (1995).
[15] G. Andresen and *et al.* (ALPHA Collaboration), Physics Letters B, **In Press**, (2010), ISSN 0370-2693.
[16] N. Madsen and *et al.* (ATHENA Collaboration), Phys. Rev. Lett., **94**, 033403 (2005).
[17] G. Gabrielse and *et al.* (ATRAP Collaboration), Phys. Rev. Lett., **89**, 233401 (2002).
[18] C. A. Ordonez and D. L. Weathers, Phys. Plasmas, **15**, 083504 (2008).